Title of Publication *Edited by*
TMS (The Minerals, Metals & Materials Society), Year

Refraction of Diffusion Fronts: Hydrogen in Y/V Bilayers-

Arndt Remhof*, Dook van Mechelen, Rinke J. Wijngaarden, Ronald Griessen

Division of Physics and Astronomy, Faculty of Sciences,
Vrije Universiteit, De Boelelaan 1081, 1081 HV Amsterdam, The Netherlands

*Present Address: Institut für Experimentalphysik/Festkörperphysik, Ruhr-Universität Bochum, D-44780 Bochum, Germany

Keywords: Solid State Diffusion, Hydrogen in Metals, Thin Films, Switchable mirrors

Abstract

Refraction and reflection, which are concepts from classical optics, have sometimes been discussed in relation to diffusive processes, such as diffusion waves.
Diffusion waves arise from an oscillatory source of particles or energy in a diffusive medium. A classical example is the oscillating temperature in the depth profile of the earth resulting from the seasonal temperature variation [1]. Diffusion waves form the basis of several new and revolutionary measurement technologies [2]. They are, however, so heavily damped that their observation is a real challenge to the experimentalist
We show that accurate information about the refraction- and reflection-like behavior of diffusion *waves* can be obtained by studying diffusion *fronts*. For this we use hydrogen in a metal as a model system and visualize its 2D migration with an optical indicator.
The similarities and dissimilarities between classical optics and *diffusion* and in particular the applicability of Snell's law to diffusive systems are discussed. We compare our measurements with numerical simulations and show that the measured diffusion *fronts* behave very much like the lines of constant phase in diffusion *waves*.

Introduction

In general, a simple model system to study the behavior of diffusion fronts and waves consists of two adjacent media with different diffusivities. A constant or an oscillatory source of particles placed close to the interface produces spherical iso-concentration lines or spherical diffusion waves that become distorted as they cross the interface. Mandelis [3] and Schendeleva [4] recently carried out extensive theoretical studies of parabolic diffusion wave fields at linear and planar interfaces. Experimentally, this problem has been studied so far for photon density waves in turbid media [5]. The behavior of the diffusion wave could, however not be studied with sufficient accuracy to discuss quantitatively the validity of Snell's law. Similar studies have been carried out on reaction-diffusion systems that are described by differential equations more complicated than diffusion [6,7]. Within this work we consider a simple purely diffusive system that allows detailed and accurate measurements of the influence of a boundary on diffusing particles. For this we choose the fast diffusion of hydrogen in thin Y/V bilayers. In this two-dimensional solid-state system the effective H mobility is varied locally by adjusting the Y/V thickness ratio [8].
Recently, we demonstrated that a thin Y coating can be used as an optical indicator to visualize hydrogen migration in opaque vanadium films. The indicator method is a further development of the optical method presented by Den Broeder et al. [9] to monitor the *lateral* migration of or

hydrogen in Y, exploiting the intrinsic concentration dependent optical properties of the YH system [10]. Thus spatial and temporal concentration variations within a Y– H film can easily be monitored optically. Especially the diffusion front separating the coexisting α- and β-phases is clearly identified as a discontinuous change in transmission and reflection. In Y the phase boundary of the *hcp* α-phase is $c_{\alpha,max}$ = 0.2 H/Y and that of the *fcc* β-phase is $c_{\beta,min}$= 1.7 H/Y. Therefore the two phases are separated by a large miscibility gap of Δc = 1.7 H/Y. The indicator technique uses the intrinsic optical properties of a thin Y layer covering the material under investigation, in the present case a V film, to visualize the H migration in the sample. The method makes use of the fact that: (i) the H-diffusion coefficient in V is orders of magnitude higher than the one in Y and (ii) the hydrogen affinity of V is low compared to the hydrogen affinity of Y. Consequently H migrates mainly via the V layer to the Y indicator. Since the total H flux through a sample scales with its cross section, the effective H mobility can be tuned via the V/Y thickness ratio. Using shadow masks during deposition, it is possible to vary the V/Y thickness ratio locally and to create, for example, single thickness steps or more complex planar structures.
The experimental results are compared with numerical calculations. Two different approaches are realized. First we solve the diffusion equation

$$\frac{\partial c}{\partial t} = D\Delta c \qquad (1)$$

whith a finite element technique. The resulting flux of particles J is given by

$$\vec{J} = -D\nabla c \qquad (2)$$

The only input parameters are the two different diffusivities of the two media and the initial hydrogen concentration. Here the concentration is a *continuous* variable.
Second, we consider the *individual* hydrogen atoms as random walkers. Here the input parameters are the diffusion length and the dwell time in the adjacent media. Both simulations reproduce the experimental results quite well.

Sample Preparation and Characterization

The samples are prepared by means of e-gun evaporation in an ultra high vacuum system (background pressure < 10-9 mbar). A typical sample consists of a V layer deposited at a rate of 0.05 nm/s onto a polished amorphous quartz substrate (Suprasil 1, Heraeus), kept at room temperature. With the help of shadow masks we can locally vary the thickness of the layer and thereby create V patterns as single steps or stripes. Subsequently, the V layer is covered with a 50 nm thick Y layer, serving later on as an optical indicator for hydrogen diffusion. Finally, to enable hydrogen uptake the samples are partially covered with a 10 nm to 15 nm thick Pd layer, deposited under the same conditions. Again shadow masks allow to pattern the Pd cover layer. Usually single Pd dots of 0.5 mm diameter or stripes with a typical width of 1 - 2 mm are used. In ambient air the uncovered parts of the sample oxidize superficially. This natural oxide layer prevents the sample from further corrosion and blocks hydrogenation. The deposition process (thickness, growth rate) of the metallic layers is monitored *in-situ* by means of a water cooled quartz microbalance. Prior to hydrogenation the sample thickness is measured *ex situ* by profilometry and by Rutherford backscattering (RBS). Furthermore, RBS is used to check for chemical impurities and to detect eventual alloy formation at the interfaces. The RBS spectra show well defined layers, no intermixing at the interfaces and no chemical contaminations. The

thickness of the natural oxide layer that forms in ambient air on the uncovered part of the yttrium layer is determined to be 15 nm.

The hydrogen gas loading is carried out in a gas-tight stainless steel cell, equipped with a gas handling system, temperature control and optical windows. The gas loading cell is mounted onto the positioning table of an optical microscope (Olympus BX60F5). Illuminated by a white lamp, optical reflection changes are monitored by means of a three-CCD red-green-blue (RGB) colour camera (Sony DXC--g50P). This camera possesses a CCD chip with an array of 582 by 782 pixels. For the small magnifications used in this study, the spatial resolution of $2 \times 2\ \mu m^2$ is determined by the pixel size of the camera.

Experimental Results and Discussion

The indicator method is demonstrated on a sample consisting of two V stripes with respective thicknesses of 50 and 75 nm, as shown in Fig.1a.

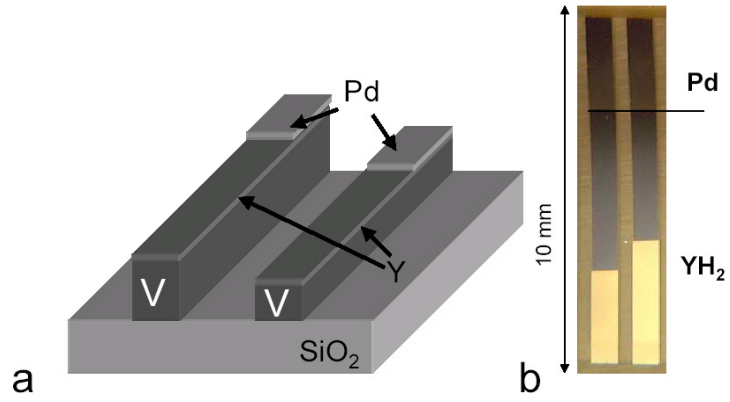

Fig.1 (a) Schematic sample design. Y covered V stripes ($1\times10mm^2$) with varying V thickness are used to demonstrate the tunability of the effective mobility of the diffusion front. (b) Photography of a 2-stripe-sample loaded in a H_2 atmosphere of 1mbar for 10^4s. H uptake occurs via the Pd covered part of the stripes. The influence of the V thickness on the progress of the H diffusion front is clearly visible.

Fig. 1b depicts a photographic image of the sample after exposure to a hydrogen atmosphere of 1 mbar at 200C for 10^5 s. Both strips are partially hydrogenated. The highly reflecting α phase appears more bright than the β-phase. The front separating phases in the Y indicator extends roughly 5 mm away from the Pd border in the thicker stripe, while it only extends 4 mm from the Pd border in the thinner film. Obviously, the effective mobility of the hydrogen in the bilayer can be tuned by the V/Y thickness ratio.
Figure 2 shows the effect on the shape of an originally spherically shaped diffusion front, as it encounters a straight interface, separating two media with different effective mobility. Experimentally this is realized by two different V thicknesses at both sides of the interface. The sample has been exposed 13000s to a hydrogen atmosphere of 1 bar at room temperature. In the upper half of the sample the effective mobility exceeds the effective mobility of the lower half by a factor of 5. H enters the sample via the circular Pd dot (0.5 mm diameter), which can be seen at he lower right corner of the picture. In the lower half of the sample the original,

spherical shape of the front can still be seen. Close to the interface the diffusion front gets distorted and an overall mushroom like pattern forms.

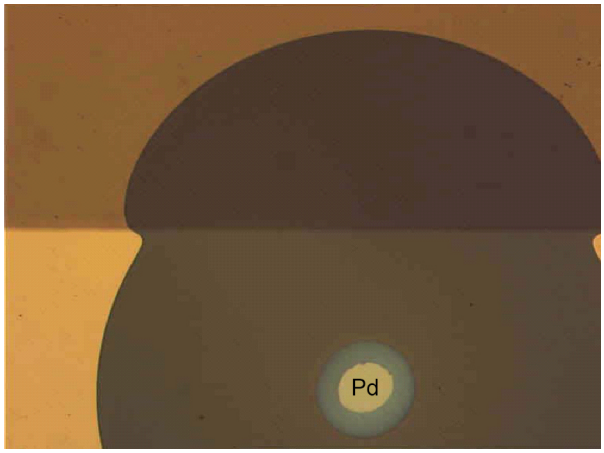

Fig.2: Lateral H diffusion in a sample with a step like variation of the V thickness. Note the distortion close to the interface. The photograph depicts a 5.6×4.5 mm2 area of the sample loaded in a H_2 atmosphere of 1bar for 32min.

The temporal evolution of the front is depicted in figure 3. The numbers in figure 3, which label the fronts, is the time elapsed (in min.) since the start of the hydrogen exposure.

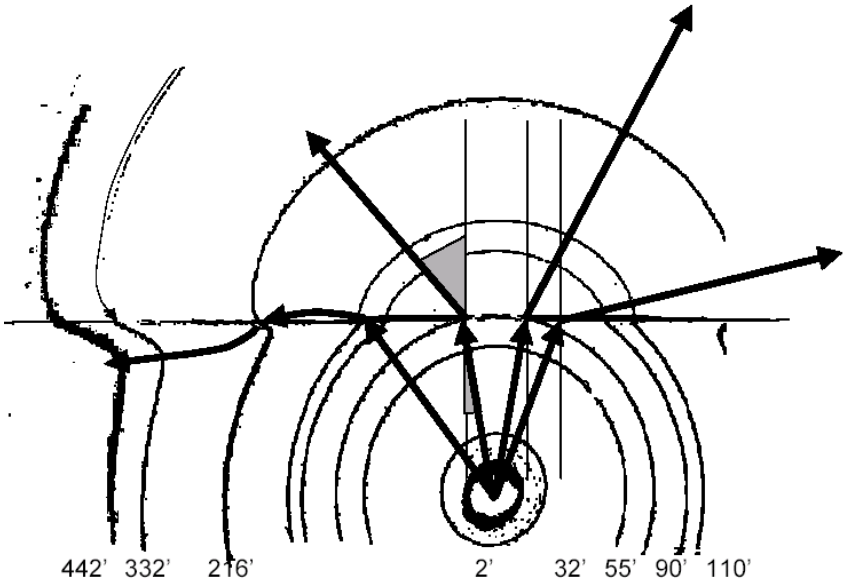

Fig.3 Temporal evolution of the diffusion front in a sample with a step like variation of the V thickness loaded in a hydrogen atmosphere of 1bar. The time indicated at the fronts is given in minutes. Superimposed are some flux lines, which intersect the diffusion front perpendicular. For small angels, the "refraction" of the flux lines follows Snell's law, indicated by the gray triangles.

Treating the fonts like optical wave fronts, "rays" can be constructed that intersect the fronts perpendicularly. A few examples of these rays are superimposed on the fronts in fig.3.
For small angles, Snell's law is fulfilled, where the square root of the ratio of the respective effective mobilities K_i plays the role of the refractive index.

$$\frac{\sin\alpha}{\sin\beta} = \sqrt{\frac{K_1}{K_2}} \qquad (3)$$

However, if sin(β) approaches unity, the `refracted' diffusion front becomes distorted.

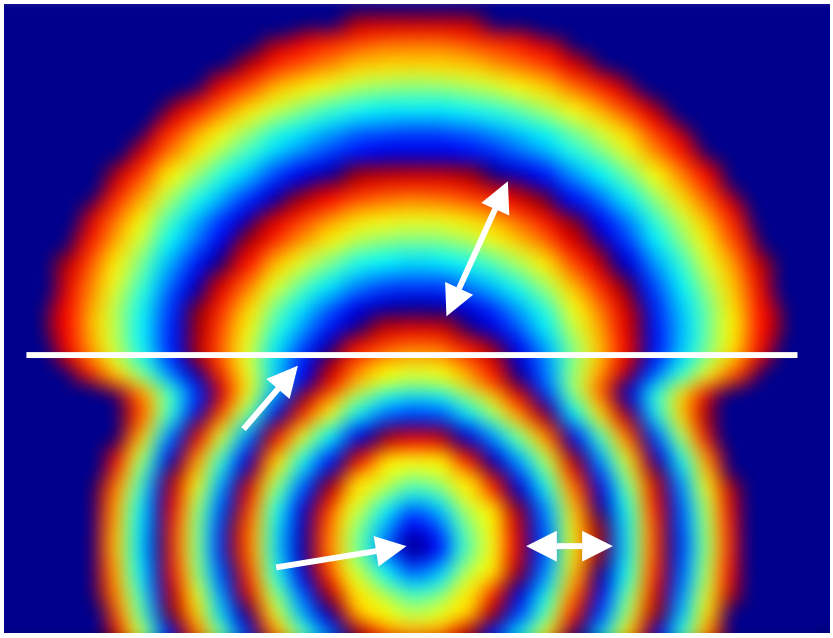

Fig.4 Numerical simulation of a sinusoidal diffusion wave originating from a point source. Lines of constant phase are expressed by identical colors. Note the change of the wavelength as the wave crosses the interface, separating two media with different diffusivities (D_1/D_2=5) The lines of constant phase behave like the temporal development of the expanding diffusion front in fig.2.

We compare now our experimental results with numerical simulations where the equations 1 and 2 are solved with a finite element technique. The only input parameters are the two different diffusivities and the hydrogen concentration below the Pd dot. At the start of the simulation the concentration is zero everywhere.
A diffusion wave with a sinusoidal oscillatory source term at the Pd dot is situated in medium1, characterized by the diffusivity D_1. We find that the oscillatory source generates a circular wave with wavelength λ_1. As soon as the wave encounters the interface, the wave field gets distorted. In the second medium, characterized by a diffusivity D_2 (D_2=5D_1), the wavelength increases to λ_2. The observed ratio of λ_1/λ_2 is given by

$$\frac{\lambda_1}{\lambda_2} = \sqrt{\frac{D_1}{D_2}} \qquad (4)$$

which is, like eqn.3, a formulation of Snell's law, where the ratio of the square roots of the diffusivities plays the role of the refractive index.
In fig.4 we plot the phase difference between the source and the foremost zero-crossing of the concentration. Identical colors represent identical phase (modulo 2π). The lines of constant phase thus represent iso-concentration lines. These calculated lines reproduce the diffusion front monitored in our experiment. Above a critical angle, a total-reflection-like regime is observed (see fig. 3), where all flux lines merge. Details of these simulations and a more in depth discussion are given in reference [11].

In a second approach we simulate the individual diffusion of the H atoms in the Y/V bilayers as random walkers. Analogue to the first simulation, at the start the concentration is zero everywhere, except at one point indicated by the dot (see Fig.5). From this point source walkers enter the medium of the lower diffusivity. For each step, they walk in randomly chosen directions. Fig.5 displays the distribution of the random walkers after a time much larger than the average time of one step. As can be seen, the diffusivity of the lower half plane is smaller than in the upper half plane. The diffusion front of the simulation using random walkers resembles to a large extent the H diffusion experiment (cf. Fig. 2). The physical interpretation of the random walker simulation for H diffusion in metallic bilayers is subject of current research.

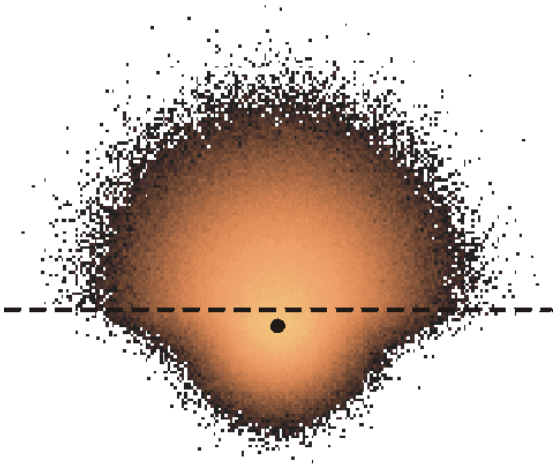

Fig.5 Simulated distribution of hydrogen atoms after diffusing randomly in two media of different diffusivities. The medium of low diffusivity in the lower half plane is separated by the dotted line from the medium of high diffusivity in the upper half plane. H atoms, simulated by random walkers, originate from the dot indicated in the lower half plane. The intensity at a given point represents the logarithm of the concentration H atoms at that point.

In conclusion we demonstrated that Y/V bilayers offer the possibility to tune and to visualize solid state diffusion in a 2D system. Numerical simulations based on individual random walkers, representing the diffusing H particles, as well as simulations that treat the H concentration as a continuous variable reproduce the experimental results quite well. The optical analogon breaks down for large angles.

Acknowledgements

We thank Jan H. Rector and Nico Koeman for the RBS measurements and technical assistance during sample preparation. We are grateful for fruitful discussions with Margarita L. Shendeleva, Sense Jan van der Molen and Bernhard Dam. This work was financially supported by the *Stichting voor Fundamenteel Onderzoek der Materie* (FOM) which is supported by the *Nederlandse Organisatie voor Wetenschappelijk Onderzoek* (NWO).

References

1. A. Sommerfeld, Partielle Differentialgleichungen der Physik (Verlag Harri Deutsch, Thun, 1978), reprint of 6th ed.
2. A. Mandelis, Phys. Today **53**, No. 08, 29 (2000), and references therein.
3. A. Mandelis, L. Nicolaides, and Y. Chen, Phys. Rev. Lett. **87**, 020801 (2001).
4. M. L. Shendeleva, Phys. Rev. B **65**, 134209 (2002);
   M. L. Shendeleva, J. Appl. Phys. **91**, 3444 (2002);
   M. L. Shendeleva, J. A. Molloy, and N. N. Ljepojevic, Appl. Phys. Lett. **80**, 1486 (2002);
   M. L. Shendeleva, Phys. Rev. E **64**, 036612 (2001).
5. M. A. O'Leary, D. A. Boas, B. Chance, and A. G. Yodh, Phys. Rev. Lett. **69**, 2658 (1992)
6. A. M. Zhabotinsky, M. D. Eager, and I. R. Epstein, Phys. Rev. Lett. **71**, 1526 (1993).
7. J. Sainhas and R. Dilão, Phys. Rev. Lett. **80**, 5216 (1998).
8. A. Remhof, S. J. van der Molen, A. Antosik, A. Dobrowolska, N. J. Koeman, and R. Griessen, Phys. Rev. B **66**, (R)020101 (2002).
9. F. J. A. den Broeder, S. J. van der Molen, M. Kremers, J. N. Huiberts, D. G. Nagengast, A. T. M. van Gogh, W. H. Huisman, N. J. Koeman, B. Dam, J. H. Rector, S. Plota, M. Haaksma, R. M. N. Hanzen, R. M. Jungblut, P. A. Duine, and R. Griessen, Nature (London) **394**, 656 (1998).
10. M. Kremers, N. J. Koeman, R. Griessen, P. H. L. Notten, R. Tolboom, P. J. Kelly, and P. A. Duine, Phys. Rev. B **57**, 4943 (1998).
11. A. Remhof, R. J. Wijngaarden and R. Griessen, Phys. Rev. Lett. **90**, 145502 (2003).